Formation control of large-scale mobile sensor networks based on semilinear parabolic system

Xueming Qian[a,b,*], Baotong Cui[b]

[a]*School of Internet of Things, Wuxi Vocational College of Science and Technology, Wuxi 214028, P.R.China*
[b]*School of Internet of Things Engineering, Jiangnan University, Wuxi 214122, P.R.China.*

Abstract

This paper is concerned with the formation control problem for a class of large-scale mobile sensor networks. The dynamic of mobile sensors are modeled by class of semilinear parabolic system, which is a class of partial differential equation(PDE) and has rich geometric family. In this model, the communication topology of agents is a chain graph and fixed. Leader feedback laws which designed in a manner to the boundary control of semilinear parabolic system allow the mobile sensors stable deployment onto planar curves. By constructing appropriate Lyapunov functional and using linear matrix inequality, several sufficient criteria are derived ensuring the mobile sensor networks to be globally asymptotically stable at the equilibrium. A simulation example is provided to demonstrate the usefulness of the proposed formation control scheme.

Keywords:
Boundary control, Formation control, Mobile sensors, Distributed parameter systems.

1. Introduction

Wireless sensor networks (WSNs) consist of a collection of sensing devices which are connected by wireless communication. A number of sensor nodes are connected in self-organized way, and collect information accurately. With the rapidly development of micro-electro-mechanical systems, sensor nodes have lower price and smaller volume than before. In the past few years, WSNs have been extensively studied and applied in military and civilian[1−2]. Especially, the capabilities of WSNs can be greatly expanded in the case of endowing nodes with mobility using mobile robots. The use of mobile sensor networks brings reduction in power consumption and costs, improved performance. Many successful applications of mobile sensor networks include environmental monitoring[3−4], target tracking[5−8], formation control[9−10], and other areas. These applications exploit mobile sensing nodes to collect information more effectively by the network. Therefore, the investigation on the cooperative control of mobile sensor networks is very important. Since a stable control scheme for mobile sensors to move cooperatively in a distributed environment is presented in [11]. A gradient climbing task in which mobile sensor networks can adapt its configuration in response to the measured environment. In [12], three distributed stable deployment algorithms based on flocking in mobile sensor networks are addressed. Also, from the view of swarm, control problem of wireless sensor networks with mobile multi-robots is discussed in [13-14]. And, formation control of mobile sensor networks has been investigated intensively. Leader-following formation control of unicycle robots is studied in [15], and a distributed nonlinear controller is proposed. A geometrical pathway in cone method is studied to achieve the formation effectively in [16]. Stabilization of geometric pattern based on Laplacian are considered in [9,10,17]. A behavior-based approach for formation maneuvers is achieved in [18], and quantized coordination algorithms are proposed in [19] for agents' deployment and rendezvous. Distributed robust H_∞ rotating consensus problem is presented in [20],

*Corresponding author

where second-order multi-agent system with mixed uncertainties and time-delay. Deployment onto a desired planar curve is investigated in [21] and [22] using coverage control algorithms and Lie group setting, respectively.

However, with the number of agent increases, the mobile sensor network would expose a continuity of system. That is to say a large number of agents is a continuum instead of particle group. In this case, the large-scale mobile sensor network can be modeled as partial differential equation(PDE). For the past few years, the research of multi-agent begin to analysis by PDEs[23−26]. In [23], the planar formation problem was solved by Liouville equation. By using a linear hyperbolic system, the stability of vehicular platoons was analyzed in [25]. A linear reaction-advection-diffusion equation as a efficient model was used in deployment onto planar curves in [26]. Moreover, the partial difference equation(PdE)[27−28] can be studied for Laplacian control in this viewpoint. It should be pointed out that the PDE-baesd model for formation control of mobile sensor networks still has little research attention.

It is, therefore, the main focus of this paper to discuss the formation control problem for an array of large-scale mobile sensor networks using a PDE-based model. We present a framework for mobile sensors deployment onto family of planar geometric curves. The dynamic of mobile sensors are modeled by semilinear parabolic system, which treat the mobile sensors as a continuum. Such a framework which implies the communication topology of agents is a chain graph and fixed. Hence, stable formation onto planar curves can be achieved by two boundary agents, which restrained boundary condition for the semilinear parabolic system. By constructing proper Lyapunov functional and employing boundary control techniques, several sufficient criteria are derived ensuring that the addressed mobile sensor networks are globally asymptotically stable. These conditions are expressed in the term of linear matrix inequality, which can be solved by the MATLAB Toolbox effectively. A simulation example is given to demonstrate the usefulness of the proposed formation control scheme.

Notations. Throughout this paper, the superscript 'T' denotes matrix transposition and the $\boldsymbol{X} > \boldsymbol{Y}$ where $\boldsymbol{X}$ and $\boldsymbol{Y}$ are symmetric matrices, means that $\boldsymbol{X} - \boldsymbol{Y}$ is positive definite. $\boldsymbol{I}$ is the identity matrix with appropriate dimensions.

2. Problem formulation and preliminaries

For formation control of large-scale mobile sensor networks, we focus on the planar deployment problem of agents. In this paper, 2-D deployment is considered two decoupled 1-D deployment problems, which are the horizontal and the vertical direction, respectively. A large number of sensing agents will be considered as a continuum by the following dynamical model

$$\begin{cases} \dfrac{\partial x_1(\alpha,t)}{\partial t} = \dfrac{\partial^2 x_1(\alpha,t)}{\partial \alpha^2} + \phi_1(x_1(\alpha,t),\alpha,t)x_1(\alpha,t), \\ \dfrac{\partial x_2(\alpha,t)}{\partial t} = \dfrac{\partial^2 x_2(\alpha,t)}{\partial \alpha^2} + \phi_2(x_2(\alpha,t),\alpha,t)x_2(\alpha,t), \end{cases} \tag{1}$$

where $(x_1(\alpha,t), x_2(\alpha,t))$ denotes the position of agent α at time t. The parameter α as the identity of each agent in a large group of mobile sensors, and $\alpha \in [0,1]$. Namely, α is an agent's index code and as the spatial variable of semilinear parabolic system for the group's collective dynamics. $\frac{\partial x_1(\alpha,t)}{\partial t}$ and $\frac{\partial x_2(\alpha,t)}{\partial t}$ refer to the horizontal and the vertical velocity of agents, respectively.

The initial conditions associated with (1) is given by

$$x_1(\alpha,0) = x_{10}(\alpha),\ x_2(\alpha,0) = x_{20}(\alpha), \tag{2}$$

and have the mixed boundary condition

$$\begin{aligned}\frac{\partial x_1(0,t)}{\partial\alpha}&=u_{01}(t),\ \frac{\partial x_1(1,t)}{\partial\alpha}=u_{11}(t),\\ \frac{\partial x_2(0,t)}{\partial\alpha}&=u_{02}(t),\ \frac{\partial x_2(1,t)}{\partial\alpha}=u_{12}(t),\end{aligned}\tag{3}$$

where $u_{01}(t), u_{02}(t), u_{11}(t)$ and $u_{12}(t)$ are the control input.

Nonlinear functions $\phi_i(\alpha,t), i=1,2$ are of class C^1 and may be unknown. These functions satisfy

$$|\phi_i(x_i(\alpha,t),\alpha,t)|\le\phi_M,\tag{4}$$

for constant bound $\phi_M\ge 0$.

Let $\boldsymbol{x}(\alpha,t)=[x_1(\alpha,t),\ x_2(\alpha,t)]^{\mathrm{T}},\ \boldsymbol{\phi}(\boldsymbol{x}(\alpha,t),\alpha,t)=\mathrm{diag}[\phi_1(x_1(\alpha,t),\alpha,t),\ \phi_2(x_2(\alpha,t),\alpha,t)]$, $\boldsymbol{u}_0(t)=[u_{01}(t),u_{02}(t)]^{\mathrm{T}},\boldsymbol{u}_1(t)=[u_{11}(t),u_{12}(t)]^{\mathrm{T}},\boldsymbol{x}(\alpha,0)=[x_1(\alpha,0),\ x_2(\alpha,0)]^{\mathrm{T}}$, $\boldsymbol{x}_0(\alpha)=[x_{10}(\alpha),\ x_{20}(\alpha)]^{\mathrm{T}},\boldsymbol{x}(0,t)=[x_1(0,t),\ x_2(0,t)]^{\mathrm{T}},\boldsymbol{x}(1,t)=[x_1(1,t),\ x_2(1,t)]^{\mathrm{T}}$.

Then, the system (1) can be rewritten into a compact form as

$$\frac{\partial\boldsymbol{x}(\alpha,t)}{\partial t}=\frac{\partial^2\boldsymbol{x}(\alpha,t)}{\partial\alpha^2}+\boldsymbol{\phi}(\boldsymbol{x}(\alpha,t),\alpha,t)\boldsymbol{x}(\alpha,t).\tag{5}$$

The initial and mixed boundary condition of system (5) as follows:

$$\boldsymbol{x}(\alpha,0)=\boldsymbol{x}_0(\alpha),\tag{6}$$

$$\frac{\partial\boldsymbol{x}(0,t)}{\partial\alpha}=\boldsymbol{u}_0(t),\ \frac{\partial\boldsymbol{x}(1,t)}{\partial\alpha}=\boldsymbol{u}_1(t),\tag{7}$$

where $\frac{\partial\boldsymbol{x}(i,t)}{\partial\alpha}$ means $\frac{\partial\boldsymbol{x}(\alpha,t)}{\partial\alpha}\big|_{\alpha=i}, i=0,1$.

A large group of agents as a continuum by system (5), two boundary agents are designated a crucial role. Index $\alpha=1$ is the leader agent and $\alpha=0$ is the anchor agent, the rest of index $0<\alpha<1$ are the follower agents. A decentralized communication topology is given, which is a chain graph. All the agents utilize only local information that is nearest-neighbor in terms of the fixed communication structure.

To give our main results, we introduce the following definition and lemmas.

Definition 1 The semilinear parabolic system (5) is said to be globally asymptotically stable at the equilibrium curve $\bar{\boldsymbol{x}}(\alpha)$, if

$$\lim_{t\to+\infty}\|\boldsymbol{x}(\alpha,t)-\bar{\boldsymbol{x}}(\alpha)\|=0$$

holds.

Definition 1 indicates $\lim\limits_{t\to+\infty}\boldsymbol{x}(\alpha,t)=\bar{\boldsymbol{x}}(\alpha)$. In other words, large-scale mobile sensor networks will be gradually converge onto the formation which is equilibrium curve $\bar{\boldsymbol{x}}(\alpha)$.

Lemma 1 (Poincaré Inequality[29]). For any $z(\xi)$, continuously differentiable on $[0,1]$. Then, the following inequality holds:

$$\int_0^1\boldsymbol{z}^2(\xi)\mathrm{d}\xi\le 2\boldsymbol{z}^2(1)+4\int_0^1\left(\frac{\mathrm{d}\boldsymbol{z}(\xi)}{\mathrm{d}\xi}\right)^2\mathrm{d}\xi.$$

Lemma 2 (Barbalat's Lemma[30]) Let $f(t)$ be a non-negative function defined on $[0,+\infty)$. If $f(t)$ is Lebesgue integrable on $[0,+\infty)$ and is uniformly continuous on $[0,+\infty)$, then $\lim\limits_{t\to+\infty}f(t)=0$.

Our main goal in this paper is to deploy a large number of agents in which continuum model onto various planar curves by designing the controllers of two boundary agents $\boldsymbol{u}_0(t)$ and $\boldsymbol{u}_1(t)$. Hereinafter, the 2-D formation problem could be investigated in two aspects. For one thing, what type of the plane curve as a formation can be reached under the PDE dynamical model? For another thing, how to design the boundary controllers such that a large number of mobile agents reaches the formation stably?

First of all, we focus on the way to acquire the curve of formation.

3. Plane curve of formation design

As mentioned above, the large-scale mobile agents are governed by semilinear parabolic system (5). Those agents are capable of reaching the formation correspond to the nonzero equilibrium curves of (5). It is not difficult to draw that the equilibrium equation of (5) is second ordinary differential equation

$$\frac{\mathrm{d}^2\bar{\boldsymbol{x}}(\alpha)}{\mathrm{d}\alpha^2} + \boldsymbol{\phi}(\alpha)\bar{\boldsymbol{x}}(\alpha) = 0, \tag{8}$$

where $\bar{\boldsymbol{x}}(0)$ and $\bar{\boldsymbol{x}}(1)$ are given.

In fact, (8) is a vary-coefficient differential equation, due to $\boldsymbol{\phi}(\alpha)$ included in the coefficient of state. The challenging problem can be solved through method of power series. According to the solution of (8), rich types of formation would be included in family of equilibrium curves.

For the sake of concise analysis, we consider the homogeneous parabolic system in the following:

$$\frac{\partial \boldsymbol{x}(\alpha,t)}{\partial t} = \frac{\partial^2 \boldsymbol{x}(\alpha,t)}{\partial \alpha^2} + \boldsymbol{\phi}\boldsymbol{x}(\alpha,t). \tag{9}$$

where $\boldsymbol{\phi} = \mathrm{diag}[\phi_1, \phi_2]$ and all the agents using the same constant $\boldsymbol{\phi}$. The deployment planar curves desired correspond to the nonzero equilibrium curves of (9). And, curves of deployments are satisfy the two-point boundary value problem

$$\frac{\mathrm{d}^2\bar{\boldsymbol{x}}(\alpha)}{\mathrm{d}\alpha^2} + \boldsymbol{\phi}\bar{\boldsymbol{x}}(\alpha) = 0 \tag{10}$$

where $\bar{\boldsymbol{x}}(\alpha) = [\bar{x}_1(\alpha),\ \bar{x}_2(\alpha)]^{\mathrm{T}}$ with $\bar{\boldsymbol{x}}(0)$ and $\bar{\boldsymbol{x}}(1)$ known. This allows for a general family of equilibrium curves selected by setting constant coefficients $\boldsymbol{\phi}$. However, the equilibria depicted by (10) may be open loop unstable. Thus, control of leader agent and anchor agent are vital to stabilize the deployment planar curves.

Remark 1. Our results can be easily applicable to linear reaction-advection-diffusion equation

$$\frac{\partial \boldsymbol{z}(\alpha,t)}{\partial t} = \frac{\partial^2 \boldsymbol{z}(\alpha,t)}{\partial \alpha^2} + \boldsymbol{b}\frac{\partial \boldsymbol{z}(\alpha,t)}{\partial \alpha} + \boldsymbol{\lambda}\boldsymbol{z}(\alpha,t), \tag{11}$$

with constant coefficient vector $\boldsymbol{b}$ and $\boldsymbol{\lambda}$ under the mixed boundary conditions (6).

We change variables $\boldsymbol{z}(\alpha,t) = \boldsymbol{w}(\alpha,t)e^{-\frac{1}{2}\boldsymbol{b}\alpha}$. This leads to

$$\frac{\partial \boldsymbol{w}(\alpha,t)}{\partial t} = \frac{\partial^2 \boldsymbol{w}(\alpha,t)}{\partial \alpha^2} + \boldsymbol{\phi}\boldsymbol{w}(\alpha,t), \tag{12}$$

where $\boldsymbol{\phi} = \boldsymbol{\lambda} - \frac{\boldsymbol{b}^2}{4}$.

The nonzero equilibrium curves of (12) satisfy

$$\frac{\mathrm{d}^2\bar{\boldsymbol{w}}(\alpha)}{\mathrm{d}\alpha^2} + \boldsymbol{\phi}\bar{\boldsymbol{w}}(\alpha) = 0. \tag{13}$$

It is obvious that (12) and its nonzero equilibrium curves have the same form as (9) and (10). We can solve the reaction-advection-diffusion equation (11) and parabolic system (9) in the same way. Besides that, it is easy to see that (9) has only one parameter vector, but equivalent to (11) which has two parameter vectors. One parameter will be more simple than two parameters selected when setting the family of desired deployment planar curves.

For the formation of large-scale mobile sensor networks, we introduce decoupled 1-D PDE model for vertical and horizontal direction, which yields two deployments $\bar{x}_1(\alpha)$ and $\bar{x}_2(\alpha)$. Hence, the planar curve can be described in vector form as

$$\begin{bmatrix} \bar{x}_1(\alpha) \\ \bar{x}_2(\alpha) \end{bmatrix} = \begin{bmatrix} a_1 & a_2 \\ a_3 & a_4 \end{bmatrix} \begin{bmatrix} \psi_1(\alpha) \\ \psi_2(\alpha) \end{bmatrix}, \tag{14}$$

where constants a_1, a_2, a_3, a_4 are deployment coefficients, which are picked by user to generate a desired deployment. $(\psi_1(\alpha), \psi_2(\alpha))$ are basis functions connect with the solutions of (11). There are rich family of planar curves will be exhibited employing basis functions. According to the value of ϕ_i, the basis functions are categorized in Table 1. We can design the planar formation by selecting the basis functions of all the agents.

Table 1. Basis functions for 1-D deployment curves of semilinear parabolic system.

ϕ_i Value	Basis Functions $(\psi_1(\alpha),\ \psi_2(\alpha))$
$\phi_i = 0$	$(1, \alpha)$
$\phi_i > 0$	$(\cos(\theta_i\alpha), \sin(\theta_i\alpha)), \quad \theta_i = \sqrt{\phi_i}$
$\phi_i < 0$	$(e^{-\sigma_i\alpha}, e^{\sigma_i\alpha}), \quad \sigma_i = \sqrt{-\phi_i}$

Remark 2. When the PDE model are different in each dimension, the planar deployment curve can be written as

$$\begin{aligned} \begin{bmatrix} \bar{x}_1(\alpha) \\ \bar{x}_2(\alpha) \end{bmatrix} = & \begin{bmatrix} a_1 & a_2 \\ 0 & 0 \end{bmatrix} \begin{bmatrix} \psi_1(\alpha) \\ \psi_2(\alpha) \end{bmatrix} \\ & + \begin{bmatrix} 0 & 0 \\ a_3 & a_4 \end{bmatrix} \begin{bmatrix} \psi_3(\alpha) \\ \psi_4(\alpha) \end{bmatrix} \end{aligned}$$

where $(\bar{x}_1(\alpha), \bar{x}_2(\alpha))$ and $(\bar{x}_3(\alpha), \bar{x}_4(\alpha))$ are basis functions for the vertical and horizontal direction, respectively. By utilizing this clue and employing PDE-based approach, some new results can be obtained in another paper.

For presentation convenience, we denote

$$\begin{aligned} & A = \begin{bmatrix} a_0 & a_1 \\ a_2 & a_3 \end{bmatrix}, Q = \begin{bmatrix} c_1 \\ c_2 \end{bmatrix}, \ S = \begin{bmatrix} b_1 & 0 \\ 0 & b_2 \end{bmatrix}, \\ & T = \begin{bmatrix} 1 & d \\ 0 & 1 \end{bmatrix}, \ R = \begin{bmatrix} \cos\vartheta & \sin\vartheta \\ -\sin\vartheta & \cos\vartheta \end{bmatrix}, \\ & \boldsymbol{\psi}(\alpha) = [\psi_1(\alpha),\ \psi_2(\alpha)]^{\mathrm{T}}. \end{aligned}$$

Then (13) can be rewritten in the compact form as

$$\bar{\boldsymbol{x}}(\alpha) = A\boldsymbol{\psi}(\alpha). \tag{15}$$

By choosing different coefficient matrix, we can also depict the deployment of mobile sensor to be translation $\bar{\boldsymbol{x}}(\alpha) = A\boldsymbol{\psi}(\alpha) + Q$, scaling $\bar{\boldsymbol{x}}(\alpha) = SA\boldsymbol{\psi}(\alpha)$, reflection $\bar{\boldsymbol{x}}(\alpha) = TA\boldsymbol{\psi}(\alpha)$ and rotation $\bar{\boldsymbol{x}}(\alpha) = RA\boldsymbol{\psi}(\alpha)$. Combining translation and scaling, a general form as following

$$\bar{\boldsymbol{x}}(\alpha) = SA\boldsymbol{\psi}(\alpha) + Q. \tag{16}$$

Also,

$$\bar{\boldsymbol{x}}(\alpha) = RSA\boldsymbol{\psi}(\alpha), \tag{17}$$

while combining rotation and scaling.

Next, it is to show that by introducing boundary control scheme, the state which is the position of mobile agents in (5) is asymptotically stable.

3.1. Formation control scheme design

To achieve a large number of mobile sensors deployment onto desired planar curve, we consider the anchor($\alpha = 0$) and leader($\alpha = 1$) agents serve as boundary control inputs. The control law of anchor as follows:

$$\boldsymbol{u}_0(t) = K_0\boldsymbol{x}(0,t) - K_0\bar{\boldsymbol{x}}(0) + \frac{\mathrm{d}\bar{\boldsymbol{x}}(0)}{\mathrm{d}\alpha} \tag{18}$$

The control law of leader is

$$\begin{aligned} \boldsymbol{u}_1(t) = & -K_1\boldsymbol{x}(1,t) + K_0\boldsymbol{x}(0,t) + K_1\bar{\boldsymbol{x}}(1) \\ & - K_0\bar{\boldsymbol{x}}(0) + \frac{\mathrm{d}\bar{\boldsymbol{x}}(1)}{\mathrm{d}\alpha} \end{aligned} \tag{19}$$

where $\frac{\mathrm{d}\bar{\boldsymbol{x}}(i)}{\mathrm{d}\alpha}$ means $\frac{\mathrm{d}\bar{\boldsymbol{x}}(\alpha)}{\mathrm{d}\alpha}\big|_{\alpha=i}$, $i = 1, 2$.

For the aim of formation deployment, we shift the equilibrium curves $\bar{\boldsymbol{x}}(\alpha)$ to the origin by curves error

$$\boldsymbol{y}(\alpha,t) = \boldsymbol{x}(\alpha,t) - \bar{\boldsymbol{x}}(\alpha), \tag{20}$$

where $\boldsymbol{y}(\alpha,t) = [y_1(\alpha,t),\ y_2(\alpha,t)]^{\mathrm{T}}$.

Consequently, the error dynamics can be expressed by

$$\frac{\partial \boldsymbol{y}(\alpha,t)}{\partial t} = \frac{\partial^2 \boldsymbol{y}(\alpha,t)}{\partial \alpha^2} + \boldsymbol{\phi}(\boldsymbol{y}(\alpha,t),\alpha,t)\boldsymbol{y}(\alpha,t), \tag{21}$$

$$\frac{\partial \boldsymbol{y}(0,t)}{\partial \alpha} = U_0(t),\ \frac{\partial \boldsymbol{y}(1,t)}{\partial \alpha} = U_1(t), \tag{22}$$

where $\frac{\partial \boldsymbol{y}(i,t)}{\partial \alpha}$ means $\frac{\partial \boldsymbol{y}(\alpha,t)}{\partial \alpha}\big|_{\alpha=i}$, $i = 0, 1$.

Substituting (19) into (6), and considering (17)-(18) leads to

$$U_0(t) = K_0\boldsymbol{y}(0,t), \tag{23}$$

$$U_1(t) = -K_1\boldsymbol{y}(1,t) + K_0\boldsymbol{y}(0,t) \tag{24}$$

In a word, we are interested in finding a formation control scheme such that a large group of mobile sensors move to the deployment curve desired. The steps of coordinates of the agents by the design procedure are listed in the following.

(1) Present the family of desired deployment curves, and decompose into two decoupled 1-D deployments on vertical and horizontal direction.
(2) Select the basis functions of desired curves on each 1-D deployment by the family of desired deployment profiles.
(3) Confirm the specific basis functions through choosing the values of coefficient ϕ_i.
(4) Pick the coefficient of basis function to generate the specific deployment profiles on vertical and horizontal direction.
(5) Implement the control laws for mobile sensor networks, including leader, anchor, and follower agents.

4. Cloesd-loop stability analysis

In this section, gradually stable converge to desired planar curves is investigated for system (4) using Lyapunov functional approach and linear matrix inequality. The analysis of cloesd-loop stability is given in the following theorem.

Theorem 1 Under the boundary control scheme (23) and (24), the system (21)with $\lambda_{\max}(\boldsymbol{\phi}_M) < \frac{1}{4}$ is globally asymptotically stable at the equilibrium curve $\bar{\boldsymbol{x}}(\alpha)$, if there exist control gain diagonal matrices K_0 and K_1, such that the following LMI holds:

$$\Psi = \begin{bmatrix} -2K_0 & K_0 \\ K_0 & -2K_1 + I \end{bmatrix} < 0. \tag{25}$$

Proof. Consider the following Lyapunov functional

$$V(t) = \int_0^1 \boldsymbol{y}^{\mathrm{T}}(\alpha,t)\boldsymbol{y}(\alpha,t)\mathrm{d}\alpha. \tag{26}$$

Taking the time derivative of $V(t)$ along the trajectories of system (21), we obtain

$$\begin{aligned}\dot{V}(t) &= 2\int_0^1 \boldsymbol{y}^{\mathrm{T}}(\alpha,t)\left[\frac{\partial^2 \boldsymbol{y}(\alpha,t)}{\partial\alpha^2} + \boldsymbol{\phi}(\boldsymbol{y}(\alpha,t),\alpha,t)\boldsymbol{y}(\alpha,t)\right]\mathrm{d}\alpha \\ &= 2\int_0^1 \boldsymbol{y}^{\mathrm{T}}(\alpha,t)\frac{\partial^2 \boldsymbol{y}(\alpha,t)}{\partial\alpha^2}\mathrm{d}\alpha \\ &\quad + 2\int_0^1 \boldsymbol{y}^{\mathrm{T}}(\alpha,t)\boldsymbol{\phi}(\boldsymbol{y}(\alpha,t),\alpha,t)\boldsymbol{y}(\alpha,t)\mathrm{d}\alpha.\end{aligned} \tag{27}$$

According to Lemma 1, we can obtain that

$$\begin{aligned}&2\int_0^1 \boldsymbol{y}^{\mathrm{T}}(\alpha,t)\frac{\partial^2 \boldsymbol{y}(\alpha,t)}{\partial\alpha^2}\mathrm{d}\alpha \\ &= 2\boldsymbol{y}^{\mathrm{T}}(\alpha,t)\frac{\partial \boldsymbol{y}(\alpha,t)}{\partial\alpha}\bigg|_0^1 - 2\int_0^1 \left(\frac{\partial \boldsymbol{y}(\alpha,t)}{\partial\alpha}\right)^{\mathrm{T}}\left(\frac{\partial \boldsymbol{y}(\alpha,t)}{\partial\alpha}\right)\mathrm{d}\alpha \\ &\leq 2\boldsymbol{y}^{\mathrm{T}}(1,t)\frac{\partial \boldsymbol{y}(1,t)}{\partial\alpha} - 2\boldsymbol{y}^{\mathrm{T}}(0,t)\frac{\partial \boldsymbol{y}(0,t)}{\partial\alpha} \\ &\quad + \boldsymbol{y}^{\mathrm{T}}(1,t)\boldsymbol{y}(1,t) - \frac{1}{2}\int_0^1 \boldsymbol{y}^{\mathrm{T}}(\alpha,t)\boldsymbol{y}(\alpha,t)\mathrm{d}\alpha.\end{aligned} \tag{28}$$

Considering the boundary control law (23) and (24), we get

$$\begin{aligned}&2\boldsymbol{y}^{\mathrm{T}}(1,t)\frac{\partial \boldsymbol{y}(1,t)}{\partial\alpha} - 2\boldsymbol{y}^{\mathrm{T}}(0,t)\frac{\partial \boldsymbol{y}(0,t)}{\partial\alpha} \\ &= 2\boldsymbol{y}^{\mathrm{T}}(1,t)\big[-K_1\boldsymbol{y}(1,t) + K_0\boldsymbol{y}(0,t)\big] - 2\boldsymbol{y}^{\mathrm{T}}(0,t)K_0\boldsymbol{y}(0,t) \\ &= -2\boldsymbol{y}^{\mathrm{T}}(1,t)K_1\boldsymbol{y}(1,t) + 2\boldsymbol{y}^{\mathrm{T}}(1,t)K_0\boldsymbol{y}(0,t) \\ &\quad - 2\boldsymbol{y}^{\mathrm{T}}(0,t)K_0\boldsymbol{y}(0,t)\end{aligned} \tag{29}$$

Then, the following holds

$$\begin{aligned}&2\int_0^1 \boldsymbol{y}^{\mathrm{T}}(\alpha,t)\frac{\partial^2 \boldsymbol{y}(\alpha,t)}{\partial\alpha^2}\mathrm{d}\alpha \\ &\leq \boldsymbol{y}^{\mathrm{T}}(1,t)(-2K_1+I)\boldsymbol{y}(1,t) + 2\boldsymbol{y}^{\mathrm{T}}(1,t)K_0\boldsymbol{y}(0,t) \\ &\quad - 2\boldsymbol{y}^{\mathrm{T}}(0,t)K_0\boldsymbol{y}(0,t) - \frac{1}{2}\int_0^1 \boldsymbol{y}^{\mathrm{T}}(\alpha,t)\boldsymbol{y}(\alpha,t)\mathrm{d}\alpha.\end{aligned} \tag{30}$$

By (4), and substituting (30) into (27) leads to

$$\begin{aligned}\dot{V}(t) \leq\ & \boldsymbol{y}^{\mathrm{T}}(1,t)(-2K_1+I)\boldsymbol{y}(1,t)\\ & + 2\boldsymbol{y}^{\mathrm{T}}(1,t)K_0\boldsymbol{y}(0,t) - 2\boldsymbol{y}^{\mathrm{T}}(0,t)K_0\boldsymbol{y}(0,t)\\ & - \frac{1}{2}\int_0^1 \boldsymbol{y}^{\mathrm{T}}(\alpha,t)\boldsymbol{y}(\alpha,t)\mathrm{d}\alpha\\ & + 2\int_0^1 \boldsymbol{y}^{\mathrm{T}}(\alpha,t)\boldsymbol{\phi}_M\boldsymbol{y}(\alpha,t)\mathrm{d}\alpha\\ \leq\ & \boldsymbol{\eta}^{\mathrm{T}}(t)\Psi\boldsymbol{\eta}(t)\\ & + (-\frac{1}{2}I + 2\boldsymbol{\phi}_M)\int_0^1 \boldsymbol{y}^{\mathrm{T}}(\alpha,t)\boldsymbol{y}(\alpha,t)\mathrm{d}\alpha, \end{aligned} \tag{31}$$

where $\boldsymbol{\eta}(t) = [\boldsymbol{y}^{\mathrm{T}}(0,t),\ \boldsymbol{y}^{\mathrm{T}}(1,t)]^{\mathrm{T}}$ and Ψ is defined in (25).

Let $\rho_1 = \lambda_{\max}(\Psi), \rho_2 = 2\lambda_{\max}(\boldsymbol{\phi}_M) - \frac{1}{2}$. From (25), it can be inferred that $\rho_1 < 0$. The choice $\lambda_{\max}(\boldsymbol{\phi}_M) < \frac{1}{4}$, we have

$$\begin{aligned}\dot{V}(t)\ & \leq \rho_1|\boldsymbol{\eta}(t)|^2 + \rho_2\int_0^1 |\boldsymbol{y}(\alpha,t)|^2\mathrm{d}\alpha.\\ & \leq \rho_1|\boldsymbol{y}(0,t)|^2 + \rho_1|\boldsymbol{y}(1,t)|^2 + \rho_2\|\boldsymbol{y}(\alpha,t)\|^2. \end{aligned} \tag{32}$$

Therefore, we get

$$\begin{aligned}& V(t) - V(0)\\ \leq\ & \int_0^t \Big(\rho_1|\boldsymbol{y}(0,s)|^2 + \rho_1|\boldsymbol{y}(1,s)|^2 + \rho_2\|\boldsymbol{y}(\alpha,s)\|^2\Big)\mathrm{d}t,\end{aligned}$$

which implies that

$$\int_0^t \Big(|\boldsymbol{y}(0,s)|^2 + |\boldsymbol{y}(1,s)|^2 + \|\boldsymbol{y}(\alpha,s)\|^2\Big)\mathrm{d}t \leq -\frac{1}{\rho}V(0)$$

where $\rho = \max\{\rho_1,\rho_2\}$.

Accordingly,

$$\int_0^t \Big(|\boldsymbol{y}(0,s)|^2 + |\boldsymbol{y}(1,s)|^2 + \|\boldsymbol{y}(\alpha,s)\|^2\Big)\mathrm{d}t \leq +\infty \tag{33}$$

In addition,it is not difficult to verify that $|\boldsymbol{y}(0,s)|^2 + |\boldsymbol{y}(1,s)|^2 + \|\boldsymbol{y}(\alpha,s)\|^2$ is uniformly continuous on $[0,+\infty)$. Therefore, we can conclude from Lemma 2 that

$$\begin{aligned}& \lim_{t\to+\infty}\|\boldsymbol{y}(\alpha,t)\| = 0,\\ & \text{if} \lim_{t\to+\infty}|\boldsymbol{y}(0,t)| = 0 \text{ and } \lim_{t\to+\infty}|\boldsymbol{y}(1,t)| = 0.\end{aligned}$$

i.e.

$$\begin{aligned}& \lim_{t\to+\infty}\|\boldsymbol{x}(\alpha,t) - \bar{\boldsymbol{x}}(\alpha)\| = 0,\\ & \text{if} \lim_{t\to+\infty}|\boldsymbol{x}(0,t) - \bar{\boldsymbol{x}}(0)| = 0 \text{ and } \lim_{t\to+\infty}|\boldsymbol{x}(1,t) - \bar{\boldsymbol{x}}(1)| = 0.\end{aligned}$$

The system (21) is globally asymptotically stable. In other words, large-scale mobile sensor networks employ the boundary control laws (18) and (19) can be gradually stable converge to a planar formation curve $\bar{\boldsymbol{x}}(\alpha)$.

Remark 3. In fact, if choose the Lyapunov functional as $V(t) = e^{\varepsilon t}\int_0^1 \boldsymbol{y}^{\mathrm{T}}(\alpha,t)\boldsymbol{y}(\alpha,t)\mathrm{d}\alpha$ where ε is a positive scalar, we can verify the system (21) is exponentially stable along the similar line of proof of Theorem 1, and the proof is omitted.

In system (5), by taking $\boldsymbol{\phi}(\boldsymbol{x}(\alpha,t),\alpha,t) = \mathbf{0}$, then the system reduces to

$$\frac{\partial \boldsymbol{x}(\alpha,t)}{\partial t} = \frac{\partial^2 \boldsymbol{x}(\alpha,t)}{\partial \alpha^2}. \tag{34}$$

That is a linear parabolic system(heat equation) also can as a model in a large agents, which depends on only nearest-neighbors. And the equilibrium curve is satisfy

$$\frac{\mathrm{d}^2\bar{\boldsymbol{x}}(\alpha)}{\mathrm{d}\alpha^2} = 0. \tag{35}$$

As pointed out in Table 1, equilibrium curve with associate to the solutions of (35) is linear in α. The formation deployment of mobile agents only onto straight line or a point.

In this case, the corollary is easily accessible from Theorem 1.

Corollary 1 Under the boundary control scheme (23) and (24), the system (34) is globally asymptotically stable at the straight line or a point $\bar{\boldsymbol{x}}(\alpha)$, if there exist control gain diagonal matrices K_0 and K_1, such that $\Psi < 0$ holds.

5. Simulation example

In this section, we present the simulation results for a variety of deployment of formation problems utilizing semilinear parabolic systems. In the following examples, we consider the deployment of mobile sensor network with $n = 10$ agents onto formation curve and the interconnection structure is dependent on discretization of (21). The boundary formation control scheme (23) and (24) are implemented by the anchor agent and leader agent. In this manner, the mobile agents parameterized in α can move to the desired planar curve.

In simulation, the initial positions of mobile agents are sampled from the Gaussian distribution $\mathcal{N}(0,1)$. Then the LMI in Theorem 1 can be solved by using MATLAB with LMI Toolbox. Accordingly, the matrices of control gain can be obtain as follows $K_0 = \begin{bmatrix} 15.8838 & 0 \\ 0 & 15.8838 \end{bmatrix}, K_1 = \begin{bmatrix} 27.7966 & 0 \\ 0 & 27.7966 \end{bmatrix}$.

Our first scenario focuses on the agents deploy to a circular formation. In Fig. 1(a), the anchor and leader guide the agents onto a circle $\bar{x}_1(\alpha) = 5\sin(2\pi\alpha), \bar{x}_2(\alpha) = 5\cos(2\pi\alpha)$, with parameter $\phi_1 = \phi_2 = 0.04\pi^2$.

Next, the formation shown in Fig 1(b) is formed using parameter $\phi_1 = -1/16$ for x_1-axis deployment and $\phi_2 = 2\pi^2$ for x_2-axis deployment. The formation of agents stabilize the curve $\bar{x}_1(\alpha) = (2/e^{-3.5} - 1)(-e^{-3.5} - 1 + 2e^{-3.5\alpha}), \bar{x}_2(\alpha) = 5\sin(\sqrt{3}\pi\alpha)$.

The examples shown above demonstrated to the flexibility of our results on Theorem 1. We now provide two simulations that using linear parabolic system (32). The following scenario shows the agents deploy to a straight line $\bar{x}_1(\alpha) = 0.85\alpha, \bar{x}_2(\alpha) = 4.6\alpha$ in Fig. 1(c).

In last example, we employ the control laws to enable the agents rendezvous at a desired point. Fig. 1(d) depicts the agents take a route to the rendezvous point (1.5,0.8), not move to it directly.

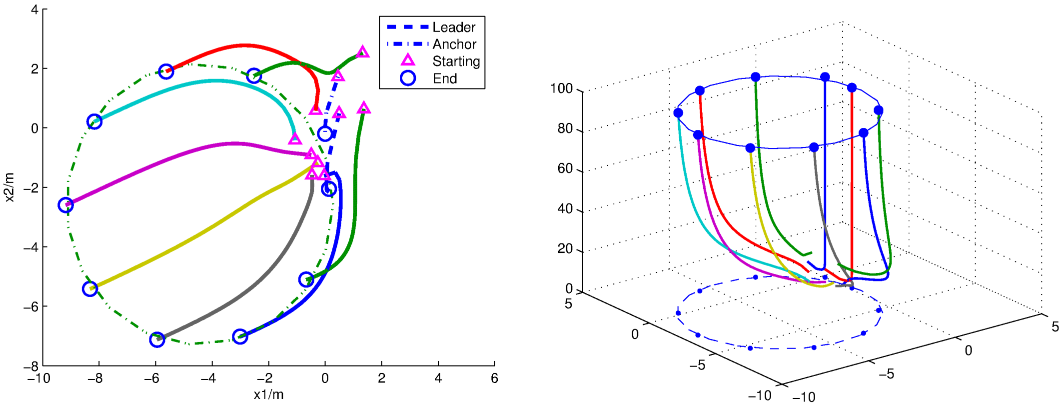

(a) Circular deployment (b) 3D view

Figure 1: Mobile sensors circular deployment

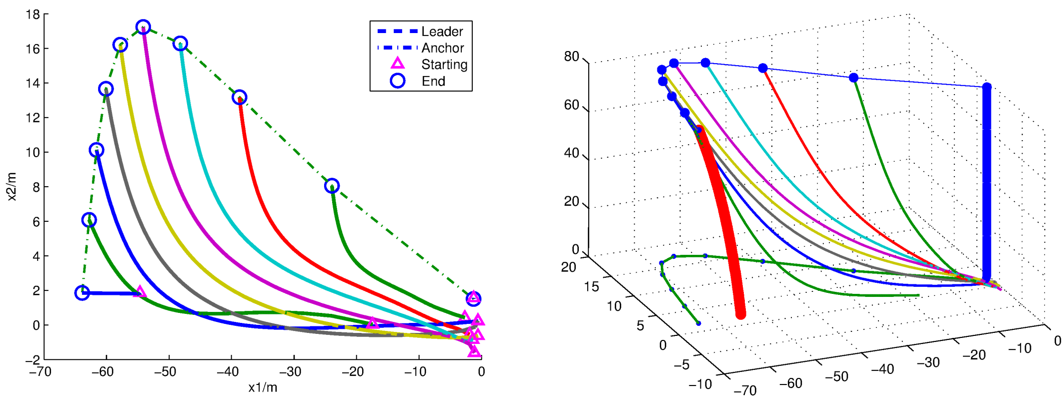

(a) Curve deployment (b) 3D view

Figure 2: Mobile sensors curve deployment

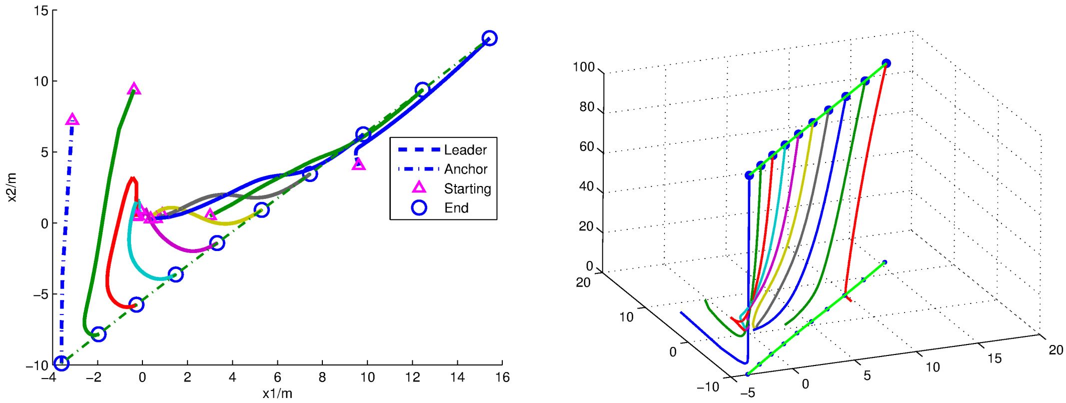

(a) Line deployment (b) 3D view

Figure 3: Mobile sensors straight line deployment

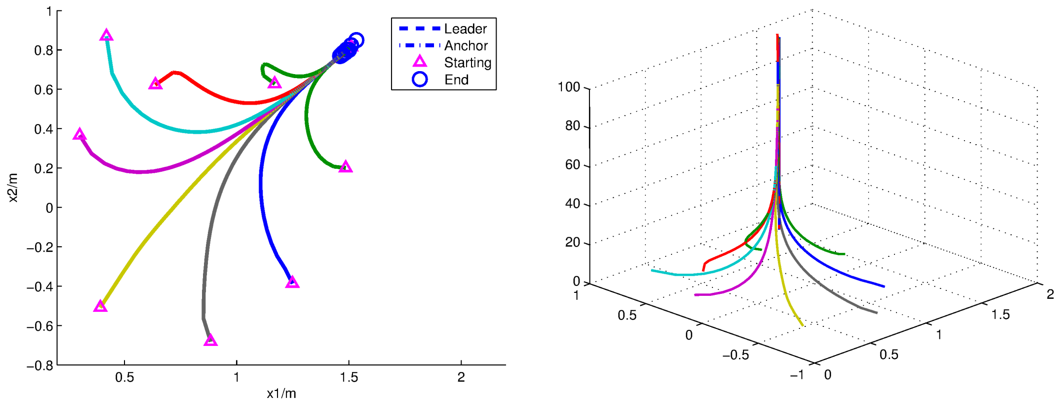

(a) Rendezvous deployment

(b) 3D view

Figure 4: Mobile sensors Rendezvous at (1.5,0.8)

6. Conclusions

In this paper, we have investigated a PDE-based model for the formation control problem of large-scale mobile sensor networks. By modeling the dynamic of a continuum of agents in terms of two decoupled semilinear parabolic system and using boundary control techniques, motion plan is given for the deployment of mobile agents onto desired formation in planar curve. In this model, the communication topology of agents is a chain graph and fixed. For this, the controllers of leader and anchor are designed to maintain a stable deployment. The control gain can be obtain in the LMI-based sufficient criteria which derived ensuring the system is globally asymptotically stable through employing Lyapunov functional method. A simulation example has been given to show the effectiveness of the proposed formation control scheme.

ACKNOWLEDGMENT

This research was supported by The Natural Science Foundation of the Jiangsu Higher Education Institutions of China (No. 17KJB510051), Qing Lan Project of the Jiangsu Higher Education Institutions (Young and Middle-aged Academic Leader(2022), Excellent Teaching Team(2020)), Soft Science Research Project of Wuxi (No. KX-20-B45), Advanced Research and Study Project for Academic Leaders of Jiangsu Higher Vocational Colleges(No. 2021GRFX068).

[1] J.A. Stankovic, Wireless Sensor Networks, IEEE Comput. Society. 41(10)(2008) 92-95.

[2] I.F. Akyildiz, W. Su, Y. Sankarasubramaniam, et al., Wireless sensor networks: a survey, Comput. Netw. 38(4)(2002) 393-422.

[3] K.M. Lynch, I.B. Schwartz, P. Yang, et al., Decentralized environmental modeling by mobile sensor networks, IEEE Trans. Robot. 24(3)(2008) 710-724.

[4] S. Susca, F. Bullo, S. Martinez, Monitoring environmental boundaries with a robotic sensor network, IEEE Trans. Contr. Syst. Tech. 16(2)(2008) 288-296.

[5] W. Chen, Y. Fu, Cooperative distributed target tracking algorithm in mobile wireless sensor networks, J. Control Theory and Appl. 9(2)(2011) 155-164.

[6] H.M. La, W. Sheng, Dynamic target tracking and observing in a mobile sensor network, Robot. and Auton. Syst. 60(7)(2012) 996-1009.

[7] S. MartíNez, F. Bullo, Optimal sensor placement and motion coordination for target tracking, Automatica. 42(4)(2006) 661-668.

[8] Z. Wu, L. Peng, L. Xie, J. Wen, Stochastic bounded consensus tracking of leader-follower multi-agent systems with measurement noises based on sampled-data with small sampling delay, Physica A. 392(4)(2013) 918-928.

[9] C. Belta, V. Kumar, Abstraction and control for groups of robots, IEEE Trans. Robot. 20(5)(2004) 865-875.

[10] J.A. Fax, R.M. Murray, Information flow and cooperative control of vehicle formations, IEEE Trans. Autom. Control. 49(9)(2004) 1465-1476.

[11] P. Ögren, E. Fiorelli, N.E. Leonard, Cooperative control of mobile sensor networks: Adaptive gradient climbing in a distributed environment, IEEE Trans. Autom. Control. 49(8)(2004) 1292-1302.

[12] Z. Tu, Q. Wang, H. Qi, et al., Flocking based sensor deployment in mobile sensor networks, Comput. Commun. 35(7)(2012) 849-860.

[13] W. Li, W. Shen, Swarm behavior control of mobile multi-robots with wireless sensor networks, J. Netw. and Comput. Appl. 34(4)(2011) 1398-1407.

[14] W. Liao, Y. Kao, Y.S. Li, A sensor deployment approach using glowworm swarm optimization algorithm in wireless sensor networks, Expert Syst. Appl. 38(10)(2011) 12180-12188.

[15] T. Liu, Z.P. Jiang, Distributed formation control of nonholonomic mobile robots without global position measurements, Automatica. 49(2)(2013) 592-600.

[16] Y. Dai, S.G. Lee, The leader-follower formation control of nonholonomic mobile robots, Int. J. Control Autom and Syst. 10(2)(2012) 350-361.

[17] G. Lafferriere, A. Williams, J. Caughman, et al., Decentralized control of vehicle formations, Syst. & control lett. 54(9)(2005) 899-910.

[18] J.R.T. Lawton, R.W. Beard, B.J. Young, A decentralized approach to formation maneuvers, IEEE Trans. Robotic. Autom. 19(6)(2003) 933-941.

[19] R. Carli, F. Bullo, Quantized coordination algorithms for rendezvous and deployment, SIAM J. Control and Optim. 48(3)(2009) 1251-1274.

[20] P. Li, K. Qin, M. Shi, Distributed robust H_∞ rotating consensus control for directed networks of second-order agents with mixed uncertainties and time-delay, Neurocomputing. (2014). DOI: 10.1016/j.neucom.2014.06.063.

[21] J. Cortes, S. Martinez, T. Karatas, et al., Coverage control for mobile sensing networks. Proceedings. ICRA'02. IEEE International Conference on Robotics and Automation. 2(2002) 1327-1332.

[22] E.W. Justh, P.S. Krishnaprasad, Equilibria and steering laws for planar formations, Syst. & Control Lett. 52(1)(2004) 25-38.

[23] E.W. Justh, P.S. Krishnaprasad, Steering laws and continuum models for planar formations, Proceedings. 42nd IEEE Conference on Decision and Control. 4(2003) 3609-3614.

[24] A. Sarlette, R. Sepulchre, A PDE viewpoint on basic properties of coordination algorithms with symmetries, Proceedings of the 48th IEEE Conference on Decision and Control, jointly with the 2009 28th Chinese Control Conference. (2009) 5139-5144.

[25] P. Barooah, P.G. Mehta, J.P. Hespanha, Mistuning-based control design to improve closed-loop stability margin of vehicular platoons, IEEE Trans. Autom. Control. 54(9)(2009) 2100-2113.

[26] P. Frihauf, M. Krstic, Leader-enabled deployment onto planar curves: A PDE-based approach, IEEE Trans. Autom. Control. 56(8)(2011) 1791-1806.

[27] G. Ferrari-Trecate, A. Buffa, M. Gati, Analysis of coordination in multi-agent systems through partial difference equations, IEEE Trans. Autom. Control. 51(6)(2006) 1058-1063.

[28] J. Kim, K.D. Kim, V. Natarajan, et al., PdE-based model reference adaptive control of uncertain heterogeneous multiagent networks, Nonlinear Analysis: Hybrid Systems. 2(4)(2008) 1152-1167.

[29] M. Krstic, A. Smyshlyaev, Boundary control of PDEs: A course on backstepping designs, Society for Industrial and Applied Mathematics, 2008.

[30] Y. Liu, Z. Wang, X. Liu, On synchronization of coupled neural networks with discrete and unbounded distributed delays, International J. Comput. Math. 85(8)(2008) 1299-1313.